

Pore structure controllable synthesis of mesoporous poly(ionic liquid)s by copolymerization of alkylvinylimidazolium salts and divinylbenzene†

Cite this: *RSC Adv.*, 2014, 4, 23389

Xuping Feng, Chenjue Gao, Zengjing Guo, Yu Zhou* and Jun Wang*

By chain radical copolymerizations of imidazolium-type ionic liquids and divinylbenzene, mesoporous poly(ionic liquid)s with tunable pore structures were synthesized. The pore size and copolymer composition involving the ionic liquid and divinylbenzene can be controlled through varying the solvents. A series of 3-alkyl-1-vinylimidazolium bromide ionic liquids with different carbon chain lengths of 4, 6, 8, 12 and 16 in the alkyl groups were used in the synthesis, which is significant for the formation of pore structures. The obtained poly(ionic liquid)s were characterized by BET, CHN elemental analysis, FT-IR and UV-vis spectra. The results indicated that poly(ionic liquid)s with varied mesopores and compositions can be facilely achieved in this system. CO₂ sorption capability and sorption-desorption cycling were tested, showing superior adsorption capability for CO₂ and durable sorption properties.

Received 8th April 2014

Accepted 15th May 2014

DOI: 10.1039/c4ra03163f

www.rsc.org/advances

1. Introduction

Poly(ionic liquids), denoted as PILs, are a kind of extensively studied polymer material synthesized by polymerization of ionic liquids (IL) monomers or copolymerization of ILs with other monomers.^{1-5,7} PILs combine some unique features of ILs and polymeric architectures. The features of ILs include negligible vapor pressure, ionicity and versatile functional groups. ILs are in liquid state at or near room temperature, while PILs with a high degree of polymerization are in solid state around room temperature.⁵ PILs can enhance the stability, processability, durability and controllability of IL species and retain most of ILs features like high ionic conductivity;^{6,7} therefore, they become a variety of new functional materials applied as thermosensitive materials,⁸ heterogeneous catalysts,^{4,9} conductive materials¹⁰⁻¹² and adsorbents.¹³ Mesoporous materials possess high surface areas, well-defined pore structure and can accelerate the interfacial mass and energy transport,¹⁴⁻¹⁶ and as a new family of mesoporous materials, mesoporous PILs (shorten as MPILs) are receiving rapidly expanding interest because of the further access to applications in catalysis and adsorption. So far, many efforts have been devoted to controlling the pore structure, morphology, chemical composition, and surface functionality for various mesoporous

materials.^{2,17-19} However, rare attention is paid on pore structure control of MPILs because it is difficult to fabricate mesoporous structures on PILs.

Recently, post-modification and one-step polymerization methods have been the major routes to prepare MPILs and control the pore structure parameters. Xiao and co-workers synthesized superhydrophobic nanoporous polymers with different solvents, onto which ILs were grafted as the catalysts for esterification, Peckmann, and Knoevenagel reactions.^{16,20} Yuan and co-workers prepared micro-/mesoporous poly(ionic liquid) materials with high specific surface area (330 m² g⁻¹) and large pore volume (1.10 cm³ g⁻¹) using a template-free ionic complexation method,² and later MPIL complexes employing multivalent carboxylic acids in diethyl ether.³ Also for catalyzing liquid-phase organic transformations, Wang and co-workers obtained several task-specific MPILs by radical copolymerization of the cross-linker divinylbenzene (DVB) and functionalized imidazolium-type ILs.^{1,21,22} Nonetheless, those MPILs usually possessed solidified mesoporous structure.

Here, we report the pore structure controlled synthesis of imidazolium-type MPILs through chain radical polymerization of IL monomers in various solvents. Solution polymerization is an easy and important synthesis method for the synthesis of polymers.²³⁻²⁵ Normally, as the reaction medium, the selected solvent is good at dissolving the monomer but it is a non-solvent for the formed polymer. Polymerization mainly takes place within the monomer-swollen progress and particles are obtained as a stable colloidal dispersion at the end of the polymerization.²⁶ Therefore, the solvents used in the synthetic media are considered to be an important factor in the formation

State Key Laboratory of Materials-Oriented Chemical Engineering, College of Chemistry and Chemical Engineering, Nanjing Tech University, Nanjing 210009, Jiangsu, P. R. China. E-mail: njutzhouyu@njtech.edu.cn; junwang@njtech.edu.cn; Tel: +86-25-83172264

† Electronic supplementary information (ESI) available. See DOI: 10.1039/c4ra03163f

of pore structures.^{17,26} In this work, various solvents, including MeOH (methanol), EtOH (ethanol), MeCN (acetonitrile), MeCN–EA (EA = ethyl acetate) mixture, and EtOH–EA–H₂O mixture, are applied in polymerization to control the mesostructure and chemical composition of the imidazolium-type MPILs prepared by copolymerizing DVB with ILs of 3-alkyl-1-vinylimidazolium bromide (alkyl = *n*-butyl, *n*-hexyl, *n*-octyl, *n*-dodecyl, or *n*-hexadecyl). Other synthetic conditions such as the initiator concentration and the molar ratio of the two monomers are also systematically investigated. CO₂ sorption capability and adsorption–desorption cycle are also tested to investigate their potential application in adsorption.^{27,28}

2. Experimental

2.1 Synthesis of imidazolium-based ILs

3-Butyl-1-vinylimidazolium bromide (VI-C4) was synthesized according to ref. 1 and the procedure was described in Scheme 1. Typically, butyl bromide (50 mmol) and 1-vinylimidazole (50 mmol) were mixed in a 100 mL flask with vigorous stirring under nitrogen atmosphere. The mixture was refluxed at 70 °C for 24 h. After reaction, the top phase was poured out, and the solid residue was washed three times with ethyl acetate and ether, finally dried at 50 °C for 12 h under vacuum. Similarly, other imidazolium-based ionic liquids with different alkyl chain length were synthesized using bromo-hexane, bromo-heptane, 1-bromodecane and 1-bromohexadecane respectively. The corresponding structure analysis was summarized as follows.

3-*n*-Butyl-1-vinylimidazolium bromide (VI-C4): ¹H-NMR (DMSO-*d*₆, δ ppm): 9.87 (1H), 8.34 (1H), 8.03 (1H), 7.37 (1H), 6.09 (1H), 5.44 (1H), 4.24 (2H), 1.80 (2H), 1.23 (2H), 0.83 (3H). ¹³C-NMR (DMSO-*d*₆, δ ppm): 135.71, 129.32, 123.74, 119.70, 109.10, 49.54, 31.70, 29.73, 29.57 (overlapped peaks), 29.55, 29.44, 29.41, 29.17, 28.98, 25.95, 22.54, 14.37.

3-*n*-Hexyl-1-vinylimidazolium bromide (VI-C6): ¹H-NMR (DMSO-*d*₆, δ ppm): 9.83 (1H), 8.35 (1H), 8.07 (1H), 7.38 (1H), 6.05 (1H), 5.41 (1H), 4.23 (2H), 1.85 (2H), 1.24 (6H), 0.84 (3H). ¹³C-NMR (DMSO-*d*₆, δ ppm): 135.67, 129.37, 123.75, 119.81, 109.11, 49.65, 31.68, 29.65, 29.61 (overlapped peaks), 29.54, 29.41, 29.41, 29.17, 28.92, 25.97, 22.52, 14.33.

3-*n*-Octyl-1-vinylimidazolium bromide (VI-C8): ¹H-NMR (DMSO-*d*₆, δ ppm): 9.86 (1H), 8.32 (1H), 8.07 (1H), 7.38 (1H), 6.08 (1H), 5.40 (1H), 4.25 (2H), 1.81 (2H), 1.20 (10H), 0.84 (3H). ¹³C-NMR (DMSO-*d*₆, δ ppm): 135.72, 129.33, 123.75, 119.72, 109.07, 49.66, 31.67, 29.67, 29.51 (overlapped peaks), 29.68, 29.45, 29.21, 29.17, 28.91, 25.97, 22.53, 14.31.

3-*n*-Dodecyl-1-vinylimidazolium bromide (VI-C12): ¹H-NMR (DMSO-*d*₆, δ ppm): 9.82 (1H), 8.31 (1H), 8.03 (1H), 7.39 (1H),

6.08 (1H), 5.41 (1H), 4.25 (2H), 1.87 (2H), 1.25 (18H), 0.83 (3H). ¹³C-NMR (DMSO-*d*₆, δ ppm): 135.74, 129.21, 123.68, 119.67, 109.04, 49.65, 31.78, 29.66, 29.51 (overlapped peaks), 29.48, 29.39, 29.27, 29.19, 28.88, 25.86, 22.57, 14.32.

3-*n*-Hexadecyl-1-vinylimidazolium bromide (VI-C16): ¹H-NMR (DMSO-*d*₆, δ ppm): 9.83 (1H), 8.37 (1H), 8.04 (1H), 7.38 (1H), 6.05 (1H), 5.45 (1H), 4.24 (2H), 1.88 (2H), 1.26 (26H), 0.84 (3H). ¹³C-NMR (DMSO-*d*₆, δ ppm): 135.78, 129.29, 123.68, 119.71, 108.93, 49.57, 31.84, 29.66, 29.52 (overlapped peaks), 29.47, 29.38, 29.31, 29.20, 28.91, 25.96, 22.55, 14.31.

2.2 Synthesis of mesoporous copolymers

The mesoporous poly(ionic liquid) was prepared through the radical co-polymerization of 3-alkyl-1-vinylimidazolium bromide (VI-C4, 6, 8, 12 and 16) and divinylbenzene (DVB),¹ as sketched in Scheme 1. In a typical synthesis, DVB (11 mmol), VI-C4 (10 mmol) and AIBN (azobisisobutyronitrile, 5.5 mmol) were dissolved in the solvent (30 mL) in a three-necked flask under nitrogen protection. The mixture was refluxed at 76 °C for 24 h with stirring. The solid was collected by filtration, washed with deionized water and ethanol and dried under vacuum at 50 °C. Various other copolymers were synthesized by varying the synthetic parameters including the solvent, initiator concentration, initial chemical compositions and the ionic liquid precursor such as using VI-C6, VI-C8, VI-C12 or VI-C16 to instead of VI-C4.

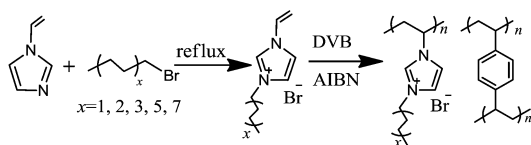
2.3 Characterization

Nitrogen sorption isotherms were measured at 77 K on a BELSORP-MINI volumetric adsorption analyzer, and the sample was outgassed in the degas port of the apparatus at 523 K for 3 h prior to testing. The BET specific surface area was calculated using adsorption data acquired at a relative pressure (P/P_0) range of 0.05–0.22 and the total pore volume was determined from the amount adsorbed at a relative pressure of about 0.99. The pore size distribution (PSD) curves were calculated from the adsorption branch of the isotherm using the Barrett–Joyner–Halenda (BJH) algorithm. The CHN elemental analysis was performed on an elemental analyzer Vario Elcube. FT-IR spectra were recorded on a Nicolet iS10 FT-IR instrument (KBr discs) in the 4000–400 cm⁻¹ region. ¹H NMR spectra were measured with a Bruker DPX 300 spectrometer at ambient temperature in D₆-DMSO using TMS as internal reference. CO₂ adsorption isotherms were measured at 298 K on a Micromeritics ASAP 2020 volumetric adsorption analyzer. SEM image was performed on a HITACHI S-4800 field-emission scanning electron microscope. UV-vis spectra were collected on the SHIMADZU UV-2600 in the region of 220–850 nm.

3. Results and discussion

3.1 MPILs synthesized by VI-C6

The mesoporous polymers are synthesized by co-polymerization of DVB and the vinylimidazolium-based ILs tethered with different length of alkyl chains. The employed ILs can be dissolved in polar solvents, such as methanol, ethanol,



Scheme 1 Synthetic procedure of mesoporous poly(ionic liquids).

acetonitrile, water and DMF (*N,N*-dimethylformamide), but partially dissolved in ethyl acetate. To get a homogeneous solution, the solvent with high solvency for both IL and DVB should be considered in the synthesis. Ethyl acetate is a good solvent for the polymerization of DVB,¹⁷ but unable to dissolve the ILs used here, while ethanol is not only excellent for dissolving the ILs but also well miscible with ethyl acetate; thus the mixture of EtOH-EA is also involved as a solvent for the copolymerization. When polymerization was performed in the absence of a solvent, no porous product can be obtained.

The effect of the solvents mentioned above on the formation of poly-VI-C6 is studied, and the result is summarized in Table 1 (entries 1–5). Nitrogen adsorption–desorption isotherms and pore size distribution curves are shown in Fig. 1A and B. All the samples give type IV isotherms. The sample prepared in acetonitrile presents a clear hysteresis loop of type H2 in the relative pressure (P/P_0) range from 0.4 to 0.9, reflecting typical mesoporous structure. The narrow pore size distribution is observed for the samples using ethanol or acetonitrile, whereas the two from methanol or MeCN-EA (15/15) demonstrate wide pore size distribution. As seen in Table 1, the obtained samples own specific surface areas from $123 \text{ m}^2 \text{ g}^{-1}$ to $512 \text{ m}^2 \text{ g}^{-1}$, which vary with the solvent type. The samples obtained from methanol, ethanol and MeCN-EA (15/15) show surface areas of $312 \text{ m}^2 \text{ g}^{-1}$, $123 \text{ m}^2 \text{ g}^{-1}$ and $124 \text{ m}^2 \text{ g}^{-1}$, respectively. Comparatively, much higher surface areas of 421 and $512 \text{ m}^2 \text{ g}^{-1}$ are observed for those from acetonitrile or EtOH-EA-H₂O (5/25/5), respectively, close to the result of the polymer material by DVB in ethyl acetate.¹⁷

DVB contains no N atom, therefore, the amount of the imidazolium-IL in the copolymer of this work is proportional to the amount of N element therein. The N contents in samples with

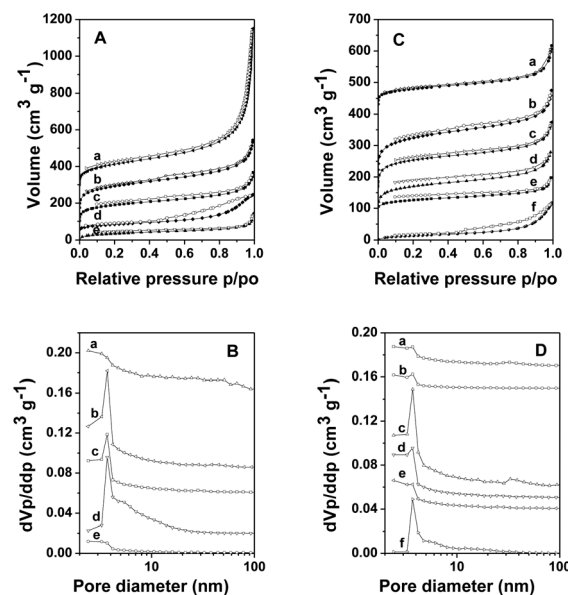


Fig. 1 Nitrogen adsorption–desorption isotherms (upper) and pore size distribution curves (bottom) of MPILs synthesized using VI-C6. (A and B) the samples prepared using (a) MeCN, (b) EtOH-EA-H₂O (5/25/5), (c) MeOH, (d) MeCN-EA (15/15) and (e) EtOH as the solvent. The adsorption isotherms for samples a, b, c and d are shifted by 500, 300, 200 and $100 \text{ cm}^3 \text{ g}^{-1}$. The pore size distribution curves for samples a, b, c and d are shifted by $0.16, 0.085, 0.06$ and $0.02 \text{ cm}^3 \text{ g}^{-1}$. (C and D) the samples prepared in mixed solvent of EtOH-EA-H₂O: (a) 0/30/5, (b) 10/20/5, (c) 15/15/5, (d) 20/5/5, (e) 25/5/5 and (f) 5/25/0. The adsorption isotherms for samples a, b, c, d and e are shifted by 430, 220, 150 and $100 \text{ cm}^3 \text{ g}^{-1}$. The pore size distribution curves for samples a, b, c and d are shifted by 0.11, 0.06, 0.04 and $0.02 \text{ cm}^3 \text{ g}^{-1}$.

Table 1 Synthetic conditions and textural properties for VI-C6-derived MPILs

Entry	IL	IL : DVB	Solvent	Volume ^a (mL)	AIBN ^b (g)	S_{BET}^c ($\text{m}^2 \text{ g}^{-1}$)	V_p^d ($\text{cm}^3 \text{ g}^{-1}$)	D_p^e (nm)	N^f (%)
1	VI-C6	1 : 1	MeOH	30	0.09	312	0.39	5.0	2.9
2	VI-C6	1 : 1	EtOH	30	0.09	123	0.19	6.3	1.7
3	VI-C6	1 : 1	MeCN	30	0.09	421	1.31	2.4	3.7
4	VI-C6	1 : 1	MeCN-EA	15/15	0.09	124	0.30	9.7	2.8
5	VI-C6	1 : 1	EtOH-EA-H ₂ O	5/25/5	0.09	512	0.61	3.7	3.3
6	VI-C6	1 : 1	EtOH-EA-H ₂ O	0/30/5	0.09	169	0.27	2.4	4.0
7	VI-C6	1 : 1	EtOH-EA-H ₂ O	10/20/5	0.09	451	0.41	3.7	2.4
8	VI-C6	1 : 1	EtOH-EA-H ₂ O	15/15/5	0.09	381	0.35	3.7	2.3
9	VI-C6	1 : 1	EtOH-EA-H ₂ O	20/10/5	0.09	264	0.28	3.7	2.2
10	VI-C6	1 : 1	EtOH-EA-H ₂ O	25/5/5	0.09	101	0.15	2.4	4.0
11	VI-C6	1 : 1	EtOH-EA-H ₂ O	5/25/0	0.09	52	0.18	3.7	3.9
12	VI-C6	2 : 1	EtOH-EA-H ₂ O	5/25/5	0.09	160	0.12	3.7	7.2
13	VI-C6	1 : 2	EtOH-EA-H ₂ O	5/25/5	0.09	455	0.19	2.4	2.2
14	VI-C6	1 : 3	EtOH-EA-H ₂ O	5/25/5	0.09	177	0.05	2.4	1.1
15	VI-C6	1 : 1	EtOH-EA-H ₂ O	5/25/5	0.01	649	0.53	3.7	2.3
16	VI-C6	1 : 1	EtOH-EA-H ₂ O	5/25/5	0.045	619	0.70	4.6	2.9
17	VI-C6	1 : 1	EtOH-EA-H ₂ O	5/25/5	0.18	486	0.57	4.7	3.6
18	VI-C4	1 : 1	EtOH-EA-H ₂ O	5/25/5	0.0900	281	0.32	3.7	5.4
19	VI-C8	1 : 1	EtOH-EA-H ₂ O	5/25/5	0.0900	491	0.38	3.7	1.4
20	VI-C12	1 : 1	EtOH-EA-H ₂ O	5/25/5	0.0900	139	0.10	3.7	2.8
21	VI-C16	1 : 1	EtOH-EA-H ₂ O	5/25/5	0.0900	130	0.06	3.7	3.4

^a Solvent volume used in the synthesis. ^b The molar ratio of ionic liquid to AIBN. ^c BET surface area. ^d Total pore volume. ^e BJH mesopore diameter calculated from the adsorption branch. ^f The nitrogen content in the final PILs.

different solvents vary from 1.7% to 3.7%, suggesting that the solvent affects the final copolymer compositions other than surface areas. The solvent seems a key to control polymerization ratio of DVB and the imidazolium-IL. The samples synthesized in acetonitrile or EtOH-EA-H₂O (5/25/5) not only offer higher surface areas but also contain larger N amounts, indicating that when these two kinds of solvents are used, large amounts of IL can be incorporated into the copolymers with high surface areas. However, the solvent acetonitrile only give a very low yield of polymer product (<10%), therefore, the mixed solvent of EtOH-EA-H₂O (5/25/5) is selected in the following studies with yields of 60–80%.

The component ratio of the solvent EtOH-EA-H₂O is altered to investigate the synthesis of MPILs. Fig. 1C and D show the nitrogen sorption isotherms and pore size distribution curves of the obtained samples. The type IV isotherms observed for all the samples evidence the typical mesoporous materials with relative narrow pore size distribution within 3–4 nm, while the exact surface area and total pore volume vary with the composition of the mixed solvent. As shown in Table 1 (entries 5 and 6), the obtained MPIL synthesized without ethanol presents surface area and total pore volume of 169 m² g⁻¹ and 0.27 m³ g⁻¹, which are much lower than those of the sample with a small amount ethanol in synthesis. Further increase of the ethanol amount with simultaneous decrease of ethyl acetate causes continuous decline in surface areas and pore volumes (Table 1, entries 7–9). The large surface areas and pore volumes relative to more amounts of ethyl acetate added in the mixed solvent agree with the previous result that ethyl acetate is a good solvent and plays a major role in polymerization of DVB.^{17,21} Besides, a small amount of water is a prerequisite to achieve abundant mesopores, because the water-free synthesized sample only present low surface area 52 m² g⁻¹ and pore volume 0.18 m³ g⁻¹. The above result indicates that the surface area and pore volume can be facily adjusted through tuning the composition of the mixed solvent EtOH-EA-H₂O, with only slight change in most probable pore sizes (Fig. 1D). Table 1 also lists the N content for the samples of entries 5–10. With moderate ethyl acetate amounts in the mixed solvent (entries 7–9), the obtained MPILs present inferior N contents around 2.3%, suggesting that the surface areas of the MPILs can be adjusted while the polymeric compositions are almost unaltered in such a solvent range. The high N content of 4.0% in the final framework of MPILs is found using either a large amount of ethanol (entry 10) or without ethanol (entry 6). Compared with other samples, the sample of entry 5 presents a considerably high N content of 3.3% and the highest surface area of 512 m² g⁻¹; therefore, EtOH-EA-H₂O with the composition 5/25/5 is suitable for achieving the high surface area MPIL with superior amount of IL incorporated in the polymer framework. It has been revealed previously that polar solutes would enhance the interactions with ILs;²⁹ also, the polar solvent ethyl acetate with polarity of 0.656 has been proved to favor the fabrication of the large surface area of the DVB-polymerized material.¹⁷ For EtOH-EA-H₂O of this work, ethanol owns lower polarity (0.520) than ethyl acetate, so the polarity of the mixed solvent increases with the added ethyl acetate. Therefore, adjustable surface areas and N contents of the obtained

copolymers by the composition of EtOH-EA-H₂O may associate with the polarity of the mixed solvent. However, insight into this possible association still needs evidence of further work.

Using EtOH-EA-H₂O (5/25/5) as the solvent, the effect of the molar ratio of VI-C6 to DVB is explored, with the nitrogen sorption isotherms for the resultant samples displayed in Fig. 2A and B. The observed type IV sorption isotherms indicate that the wide range of the VI-C6–DVB ratio can give rise to the MPIL materials. As large amounts of DVB are used, the pore size distribution of the obtained copolymers presents a narrow pore size range (Fig. 2B, curves a and b). Table 1 lists the properties of these samples (entry 12–14). The N content decreases from 7.2% to 1.1% when VI-C6–DVB ratio decreases from 2 : 1 to 1 : 3. The samples synthesized with moderate molar ratios of VI-C6 to DVB (1 : 1 and 1 : 2) exhibit large surface areas. On the contrary, the samples synthesized with either a small or a large amount of DVB all present low surface areas. Therefore, in the following syntheses, the molar ratio of the monomer IL to DVB is fixed as 1 : 1. The specific surface area is not proportional to the amount of DVB in the copolymer, implying that the incorporated IL monomer should have made significant contribution to the high surface area.

The polymerization rate is closely related to the concentration of initiator, and the influence of the amount of initiator AIBM is tested with solvent EtOH-EA-H₂O (5/25/5) at VI-

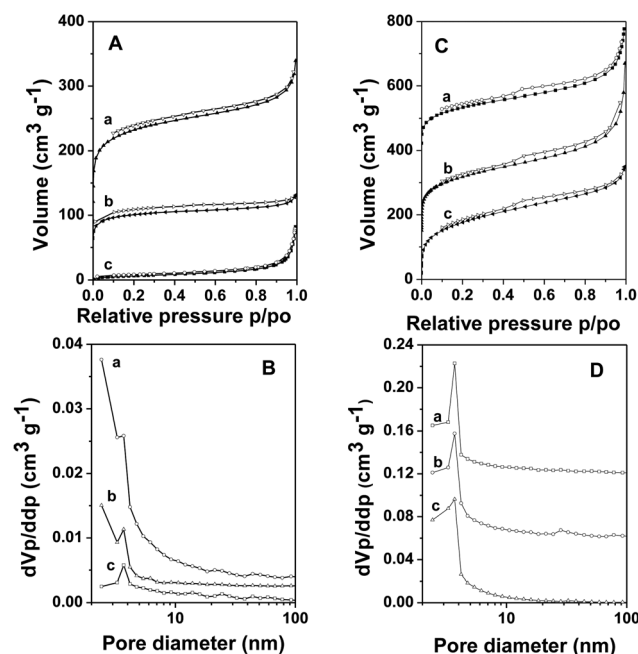


Fig. 2 Nitrogen adsorption–desorption isotherms (upper) and pore size distribution curves (bottom) of MPILs synthesized using VI-C6. (A and B) the samples prepared with different ratio of VI-C6 to DVB: (a) 1 : 2, (b) 1 : 3 and (c) 2 : 1. The adsorption isotherms for samples a and b are shifted by 100 and 50 cm³ g⁻¹. The pore size distribution curves for samples b and c are shifted by 0.0035 and 0.0025 cm³ g⁻¹. (C and D) the samples prepared with different amounts of AIBN: (a) 0.18 g, (b) 0.045 g and (c) 0.01 g. The adsorption isotherms for samples a and b are shifted by 400 and 150 cm³ g⁻¹. The pore size distribution curves for samples a and b are shifted by 0.12 and 0.06 cm³ g⁻¹.

C6 : DVB = 1 : 1. As shown in Fig. 2C and D, all the samples give similar type IV isotherms and H2 type hysteresis loops with the most probable mesopore diameter *ca.* 3.7 nm. With the increase of AIBM, the surface areas decrease while N contents increase continuously (Table 1, entries 15–17). Therefore, the pore structure and composition of MPILs can be adjusted through controlling the initiator concentration in this study.

3.2 MPILs synthesized by other ILs

The polarity of an imidazolium-IL changes with the length of the alkyl chain tethered to the imidazolium ring. According to previous literature,²⁹ the varied intermolecular interactions between the solvent EtOH–EA–H₂O of this work and the ILs with different length of alkyl chains may affect the pore structure and composition of the copolymers. Therefore, instead of VI-C6, other imidazolium-ILs with alkyl chains of VI-C4, VI-C8, VI-C12 and VI-C16 are also used for synthesizing MPILs. The nitrogen sorption results of the obtained samples are shown in Fig. 3A and B with the solvent EtOH–EA–H₂O (5/25/5) at molar ratios IL–DVB = 1 : 1 and IL–AIBN = 10 : 1. VI-C4 and VI-C8 show type IV sorption isotherms with a clear hysteresis loop of type H2 in the relative pressure (P/P_0) range from 0.4 to 0.7, similar to the result of VI-C6. The isotherms of the samples obtained from VI-C12 and VI-C16 are also type IV, with missing of the hysteresis loop. Moreover, all the samples display narrow distribution of pore size with the most probable size of 3.7 nm (Fig. 3B). The result demonstrate the validity of the present approach in fabricating MPILs using imidazolium-ILs. The detailed textural properties listed in Table 1 (entries 18–21) show that VI-C8 leads to the surface area of 491 m² g⁻¹, almost as high as that of VI-C6 (512 m² g⁻¹). Nonetheless, the N content of the former is 1.4%, lower than the latter (3.3%). The sample derived from VI-C4 has a high N content 5.4% and moderate surface area 281 m² g⁻¹. By contrast, those from VI-C12 and VI-C16 own considerable amounts of N contents of *ca.* 3.0% but with comparatively lower surface areas *ca.* 135 m² g⁻¹.

Methanol, ethanol, acetonitrile and MeCN–EA are also tried as the solvents for synthesizing MPILs with IL monomers of VI-

C4, 8, 12 and 16. The results are shown in Table S1 and Fig. S1.† For the ILs with long alkyl chains of 8, 12 and 16, the obtained MPILs presents very low surface areas using methanol, ethanol or MeCN–EA, suggesting that they are not suitable solvents for the monomers. Acetonitrile results in a moderate surface area for MPILs, but the yield is less than 10%. Similar to VI-C6, the short chain VI-C4 causes MPILs with superior surface areas and N contents, applicable to all the above-mentioned solvents.

3.3 SEM and spectral characterization

The obtained copolymers are characterized by SEM images, showing a sponge-like morphology. The morphology of these samples is similar to each other. Fig. 4 displays the SEM images of the typical sample poly(VI-C6–DVB) in entry 5 of Table 1 (SEM images of others are not shown for avoiding repetition). The primary irregular particles are in sizes of tens of nanometers. These nanoparticles are closely interacted with each other and loosely packed into large aggregates, forming a foam structure. It is owe to the varied packing of primary nanoparticles that the present approach causes the different mesostructure of copolymers compared with the previous report.¹

The copolymer materials are further characterized by FT-IR and UV-vis spectra. Fig. 5A displays the FT-IR spectra of selected samples, giving the featured vibrations related to DVB. The bands at 2900, 3024, 3060, and 3082 cm⁻¹ are due to the C–H stretching vibrations in benzene ring, while those at 2912 and 2849 cm⁻¹ are assignable to saturated and unsaturated C–H stretching vibrations. Moreover, the bands at 1605, 1494, and 1454 cm⁻¹ are attributable to the skeleton vibration of benzene ring, benzene C–H in-plane, and plane bending vibrations, respectively.^{30–33} For the imidazolium-IL moiety preserved in copolymers, the bands at 2865 cm⁻¹ is for the aliphatic C–H bending vibration, and 1573 and 1464 cm⁻¹ are indicative of the imidazole ring skeleton. In addition, the 1172 cm⁻¹ peak is the imidazole ring C–H bond plane bending vibration.^{1,34} The result allows to conclude the retaining of IL and DVB precursor in the final copolymer,¹ accordance with CHN elemental analyses. Because only the alkyl chain length is different for the employed ILs, the IR spectra of the corresponding copolymers are more or less similar to each other, merely showing slight shifts in absorption bands. The UV-vis spectra in Fig. 5B show a wide

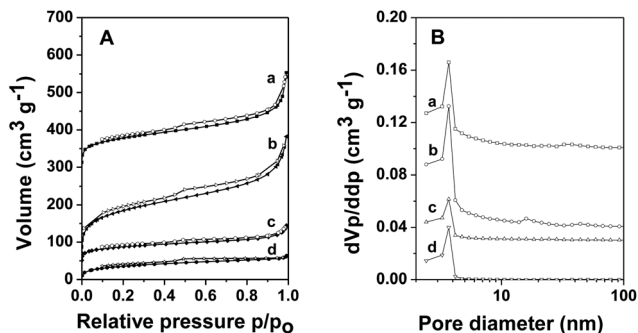


Fig. 3 Nitrogen adsorption–desorption isotherms (A) and pore size distributions (B) of the poly(ionic liquid–DVB) with different length alkyl chains (a) VI-C4, (b) VI-C8, (c) VI-C12 and (d) VI-C16. The adsorption isotherms for samples a, b and c are shifted by 300, 150 and 50 cm³ g⁻¹. The pore volumes for samples a, b and c are shifted by 0.1, 0.04 and 0.03 cm³ g⁻¹.

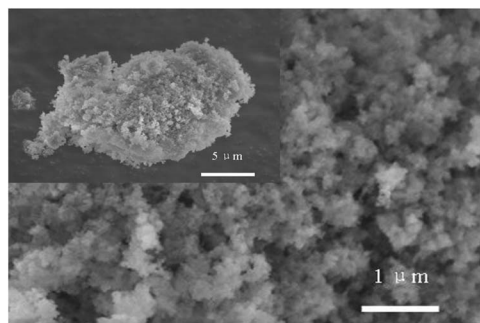


Fig. 4 SEM images of poly(VI-C6–DVB) prepared in EtOH–EA–H₂O (5/25/5); the amount of AIBN was 0.09 g (inset: SEM image of same sample).

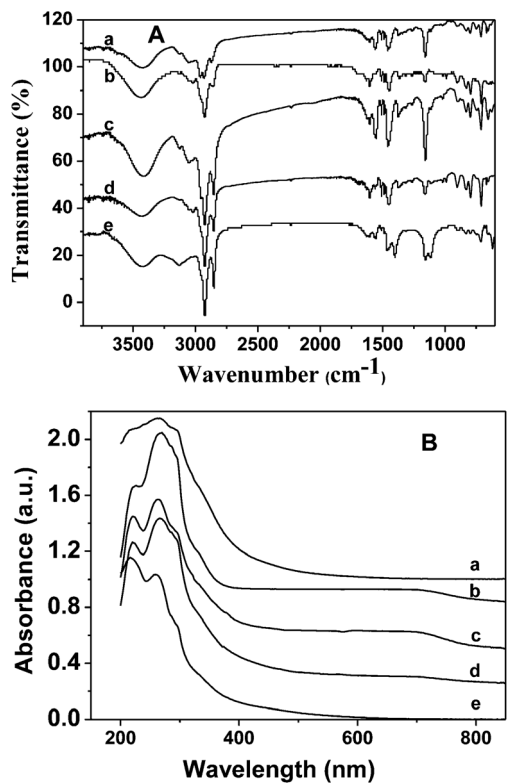


Fig. 5 (A) FT-IR spectra of poly(ionic liquid-DVB)s with different ionic liquids. (a): VI-C4; (b): VI-C6; (c): VI-C8; (d): VI-C12; (e): VI-C16. (B) UV-vis spectra of poly(ionic liquid-DVB)s with different ionic liquids. (a): VI-C8; (b): VI-C6; (c): VI-C12; (d): VI-C16; (e): VI-C4.

adsorption band ranging from 200 to 400 nm. With the increase of the alkyl chain length, a slight red shift occurs. For example, the highest peak changes from 260 to 270 nm when the alkyl chain length increases from 4 to 16. In addition, a tail adsorption ranging to 750 nm appears for the samples synthesized from VI-C12 and VI-C16 with longer alkyl chains. The above phenomenon suggests that introduction of different alkyl chains into the MPILs may affect the optical property.

3.4 CO₂ sorption

The five MPIL samples from the IL precursors of VI-C4, VI-C6, VI-C8, VI-C12 and VI-C16 are selected to be subjected to the CO₂ sorption test at 25 °C, and the results are shown in Fig. 6A. The sorption capability of the materials increases with CO₂ pressure. Generally, the copolymer incorporating more imidazolium-ILs with a larger surface area should adsorb more amount of CO₂. The lowest CO₂ sorption amount is 8 mg g⁻¹ for VI-C8-derived product due to the low N content. In contrast, the highest CO₂ sorption amount of 22 mg g⁻¹ is achieved on the sample from VI-C6 that has the highest surface area and superior N content. Compared with previously reported PILs,^{34,35} our MPIL material demonstrates superior adsorption amount of CO₂. However, the present alkylated imidazole unit in IL precursor has not been functionalized by additional basic group, so the adsorption amount of CO₂ is lower than the amino coated mesoporous materials.³⁴⁻³⁶

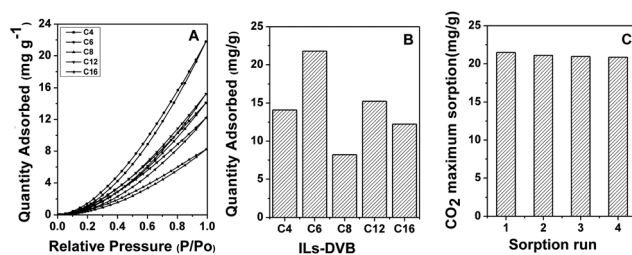


Fig. 6 CO₂ sorption property for VI-C6-DVB copolymer. (A) CO₂ adsorption-desorption isotherms; (B) maximum absorption capacity; (C) cycles of CO₂ adsorption and desorption.

Meanwhile, a five-cycle CO₂ adsorption and desorption experiment is carried out for the VI-C6-derived material with the highest adsorption amount. After each cycle, it is vacuum-dried at 80 °C to remove CO₂ and other volatile components, and then used in the next cycle. Fig. 6C shows the adsorption amount for each cycle. After five cycles, the sample remains about 97% adsorption capacity based on the fresh one, presenting a reversible sorption process and stable sorption capacity, which is the most important basis as a potential material for further practical utilization.

4. Conclusions

In summary, we have developed a very convenient one-step approach for synthesizing cross-linked polymeric IL-DVB by the conventional radical copolymerization of the cross-linker DVB and alkyl ionic liquid without adding stabilizers or surfactants. The results indicate that solvent and initiator exert significant influences on the formation of porous PILs in this strategy. PILs with varied mesopores are achieved and controlled through adjusting the solvent and initiator. Therefore, the present work provides a facile way to synthesize MPILs. Moreover, the MPILs can be applied in CO₂ sorption and the same MPIL is used in five cycles without any significant loss of sorption capability. The MPILs show potential application prospects in gas-selective adsorption, ion exchange and catalysis.

Acknowledgements

The authors thank greatly the National Natural Science Foundation of China (21136005 and 21303084), and Jiangsu Provincial Science Foundation for Youths (BK20130921).

Notes and references

- P. Zhao, Y. Leng and J. Wang, *Chem. Eng. J.*, 2012, **204**–206, 72.
- Q. Zhao, S. Soll, M. Antonietti and J. Yuan, *Polym. Chem.*, 2013, **4**, 2432.
- S. Soll, Q. Zhao, J. Weber and J. Yuan, *Chem. Mater.*, 2013, **25**, 3003–3010.
- T. Shi, J. Wang, J. Sun, Mi. Wang, W. Cheng and S. Zhang, *RSC Adv.*, 2013, **3**, 3726.
- J. Yuan and M. Antonietti, *Polymer*, 2011, **52**, 1469.

- 6 R. Sydam and M. Deepa, *J. Mater. Chem. C*, 2013, **1**, 7930.
- 7 H. Ohno, *Electrochim. Acta*, 2001, **46**, 1407–1411.
- 8 Y. Xiong, J. Liu, Y. Wang, H. Wang and R. Wang, *Angew. Chem., Int. Ed.*, 2012, **51**, 9114.
- 9 S. P. Maradur, C. Jo, D. Choi, K. Kim and R. Ryoo, *ChemCatChem*, 2011, **3**, 1435.
- 10 R. Sydam and M. Deepa, *J. Mater. Chem. C*, 2013, **1**, 7930.
- 11 M. Lee, U. H. Choi, R. H. Colby and H. W. Gibson, *Chem. Mater.*, 2010, **22**, 5814–5822.
- 12 U. H. Choi, M. Lee, S. Wang, W. Liu, K. I. Winey, H. W. Gibson and R. H. Colby, *Macromolecules*, 2012, **45**, 3974–3985.
- 13 H. Cong, B. Yu, J. Tang and X. Zhao, *J. Polym. Res.*, 2012, **19**, 9761.
- 14 Y. Zhou, M. Wan, L. Gao, N. Lin, W. Lin and J. Zhu, *J. Mater. Chem. B*, 2013, **1**, 1738.
- 15 R. Kore, B. Satpati and R. Srivastava, *Chem.–Eur. J.*, 2011, **17**, 14360.
- 16 L. Wang, J. Zhang, J. Sun, L. Zhu, H. Zhang, F. Liu, D. Zheng, X. Meng, X. Shi and F. Xiao, *ChemCatChem*, 2013, **5**, 1606.
- 17 Y. Zhang, S. Wei, F. Liu, Y. Du, S. Liu, Y. Ji, T. Yokoi, T. Tatsumi and F. Xiao, *Nano Today*, 2009, **4**, 135.
- 18 T. Chen, B. Du and Z. Fan, *Langmuir*, 2012, **28**, 15024.
- 19 M. Koebe, M. Drechsler, J. Weber and J. Yuan, *Macromol. Rapid Commun.*, 2012, **33**, 646.
- 20 F. Liu, L. Wang, Q. Sun, L. Zhu, X. Meng and F. Xiao, *J. Am. Chem. Soc.*, 2012, **134**, 16948.
- 21 Y. Leng, J. Wang and P. Jiang, *Catal. Commun.*, 2012, **27**, 101.
- 22 Y. Leng, W. Zhang, J. Wang and P. Jiang, *Appl. Catal., A*, 2012, **445–446**, 306.
- 23 Y. Wang, J. Liu and C. Xia, *Tetrahedron Lett.*, 2011, **52**, 1587.
- 24 D. Zhang, C. Zhou and R. Wang, *Catal. Commun.*, 2012, **22**, 83.
- 25 A. Pourjavadi, S. H. Hosseini, F. M. Moghaddam, B. K. Foroushanib and C. Bennett, *Green Chem.*, 2013, **15**, 2913.
- 26 S. Kawaguchi and K. Ito, *Adv. Polym. Sci.*, 2005, **175**, 299.
- 27 G. Yu, Z. Man, Q. Li, N. Li, X. Wu, C. Asumana and X. Chen, *React. Funct. Polym.*, 2013, **73**, 1058.
- 28 J. Zhu, J. Zhou, H. Zhang and R. Chu, *J. Polym. Res.*, 2011, **18**, 2011.
- 29 D. Zhang, Y. Deng, C. Li and J. Chen, *Ind. Eng. Chem. Res.*, 2008, **47**, 1995–2001.
- 30 K. H. Wu, Y. R. Wang and W. H. Hwu, *Polym. Degrad. Stab.*, 2003, **79**, 195.
- 31 X. Huang, Y. Wang, Y. Liu and D. Yuan, *J. Sep. Sci.*, 2013, **36**, 3210.
- 32 H. Chu, C. Yu, Y. Wan and D. Zhao, *J. Mater. Chem.*, 2009, **19**, 8610.
- 33 A. Pourjavadi, S. H. Hosseini and Z. S. Emami, *Chem. Eng. J.*, 2013, **232**, 453.
- 34 J. Choma, Ł. Osuchowski, M. Marszewskic and M. Jaroniec, *RSC Adv.*, 2014, **4**, 14795.
- 35 C. Xu and N. Hedin, *J. Mater. Chem. A*, 2013, **1**, 3406.
- 36 J. Ren, L. Wu and B. Li, *Ind. Eng. Chem. Res.*, 2012, **51**, 7901.